# Systemic Gene Silencing in Primary T Lymphocytes Using Targeted Lipid Nanoparticles

**Srinivas Ramishetti,[†,‡,§,▼] Ranit Kedmi,[†,‡,§,▼] Meir Goldsmith,[†,‡,§] Fransisca Leonard,[⊥] Andrew G. Sprague,[∥] Biana Godin,[⊥] Michael Gozin,[¶] Pieter R. Cullis,[#] Derek M. Dykxhoorn,[△] and Dan Peer[*,†,‡,§]**

[†]Laboratory of NanoMedicine, Department of Cell Research and Immunology, George S. Wise Faculty of Life Sciences, [‡]Department of Materials Sciences and Engineering, Faculty of Engineering, [§]Center for Nanoscience and Nanotechnology, and [¶]School of Chemistry, Tel Aviv University, Tel Aviv 69978, Israel, [⊥]Department of NanoMedicine, Houston Methodist Research Institute, Houston, Texas 77030, United States, [∥]Alnylam Pharmaceuticals, Cambridge, Massachusetts 02142, United States, [#]Department of Biochemistry & Molecular Biology, Life Science Centre, University of British Columbia, Vancouver BC V6T 1Z4, Canada, and [△]Dr. John T Macdonald Foundation, Department of Human Genetics, Hussman Institute for Human Genomics, University of Miami, Miller School of Medicine, Miami, Florida 33136, United States. [▼]S.R. and R.K. contributed equally to this work.

**ABSTRACT** Modulating T cell function by down-regulating specific genes using RNA interference (RNAi) holds tremendous potential in advancing targeted therapies in many immune-related disorders including cancer, inflammation, autoimmunity, and viral infections. Hematopoietic cells, in general, and primary T lymphocytes, in particular, are notoriously hard to transfect with small interfering RNAs (siRNAs). Herein, we describe a novel strategy to specifically deliver siRNAs to murine CD4$^+$ T cells using targeted lipid nanoparticles (tLNPs). To increase the efficacy of siRNA delivery, these tLNPs have been formulated with several lipids designed to improve the stability and efficacy of siRNA delivery. The tLNPs were surface-functionalized with anti-CD4 monoclonal antibody to permit delivery of the siRNAs specifically to CD4$^+$ T lymphocytes. *Ex vivo*, tLNPs demonstrated specificity by targeting only primary CD4$^+$ T lymphocytes and no other cell types. Systemic intravenous administration of these particles led to efficient binding and uptake into CD4$^+$ T lymphocytes in several anatomical sites including the spleen, inguinal lymph nodes, blood, and the bone marrow. Silencing by tLNPs occurs in a subset of circulating and resting CD4$^+$ T lymphocytes. Interestingly, we show that tLNP internalization and not endosome escape is a fundamental event that takes place as early as 1 h after systemic administration and determines tLNPs' efficacy. Taken together, these results suggest that tLNPs may open new avenues for the manipulation of T cell functionality and may help to establish RNAi as a therapeutic modality in leukocyte-associated diseases.

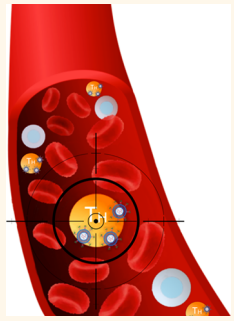

**KEYWORDS:** T lymphocytes · RNA interference · lipid-based nanoparticles · CD45

The CD4$^+$ T lymphocytes play essential roles in the immune system through their interaction with antigen-presenting cells (APCs) and the secretion of cytokines that regulate and balance the inflammatory response. Alterations in their functionality can drive a variety of immunological disorders such as inflammation, cancer, autoimmunity, and viral infections, making CD4$^+$ T cells an attractive target for a range of therapeutic interventions.[1] Recent advances in RNA interference (RNAi)-based gene silencing coupled with accumulating knowledge about the role of specific genes in immunological disorders have opened the door for the development of novel classes of gene-specific therapies. Harnessing RNAi for specific silencing of disease-relevant genes has been shown to have immense potential as a therapeutic strategy in preclinical studies across a wide variety of diseases such as cancer, inflammation, neurodegenerative diseases, and genetic disorders. However, the delivery of small interfering RNAs (siRNAs) to the disease-relevant cell types in sufficient quantities to effectively silence the target gene has remained a difficult task and has slowed their development for RNAi-based approaches. This is especially the case for cells of the immune system, including T lymphocytes that are notoriously difficult to transfect.[2−5] Although several strategies have been used to knockdown gene expression in T cells *in vitro*[6−8] and *in vivo*,[9−13] efficient and specific delivery of siRNAs to T cells in therapeutically relevant doses remains a major hurdle to the adoption of this technology for clinical applications. Recent studies have shown significant

* Address correspondence to peer@tauex.tau.ac.il.

Received for review February 25, 2015 and accepted June 4, 2015.

**Published online June 04, 2015**
**10.1021/acsnano.5b02796**

improvements in methodologies for the recognition and delivery of siRNAs to specific disease-relevant cell types. However, most of these delivery approaches have not been optimized to facilitate the intracellular trafficking of siRNAs into the cytoplasm, where they provide the targeting component of the RNA-induced silencing complex, allowing it to direct the degradation of specific mRNAs.[14]

The use of the NanoAssemblr microfluidic mixing device has greatly increased the efficacy of producing lipid nanoparticles (LNPs) containing mixtures of lipids, including fusogenic and ionizable amino lipids, to enhance both the encapsulation of siRNAs and endosomal escape once delivered to the target cells.[15] Recent studies have shown the efficacy of utilizing this technology to effectively deliver siRNA to hepatocytes.[16,17] Compared to most cell types, hepatocytes have been shown to be permissive to *in vivo* siRNA delivery, including the delivery of naked siRNAs using hydrodynamic injection.[18] Several recent *in vivo* studies have suggested that LNP-based approaches may be effective for targeting leukocytes. Novobrantseva *et al.* demonstrated gene knockdown in murine peritoneal macrophages *in vivo*,[19] while He *et al.* showed robust gene silencing in human T cells *in vitro*[20] and a moderate level of generalized (*i.e.*, not specific to any lymphocyte population) silencing in spleen and bone marrow hematopoietic tissues. These recent results suggest that these LNP formulations may facilitate siRNA delivery to immune cells and release of the siRNAs from phagosomes or endosomes into the cytoplasm, opening a new avenue in the field of leukocyte siRNA transfections.

For LNP-based siRNA delivery technology to be effectively applied for the therapeutic manipulation of gene expression in T cells, it requires an additional layer of specificity. To target specific subsets of leukocytes, an active targeting approach needs to be considered. To that end, we sought to develop a platform for the silencing of gene expression in specific populations of T cells. This approach is based on a robust and scalable ionizable LNP system. Using the NanoAssemblr, we developed LNPs that incorporate the fusogenic ionizable lipid DLin-MC3-DMA, which has been shown to be a potent lipid for siRNA delivery.[15,21] Targeted LNPs were established by coating the LNPs with monoclonal antibodies against the T cell surface CD4 receptor. Using siRNA to knockdown the cell surface tyrosine phosphatase CD45, a pan leukocyte marker, we demonstrate the capability of these monoclonal antibody (mAb)-coated LNPs to selectively target $CD4^+$ cells *in vivo* and to induce effective gene silencing. Our results confirm targeting in all leukocyte-rich organs tested: blood, spleen, lymph nodes, and bone marrow. This scalable, robust LNP-based siRNA delivery method may help to pave the way for the use of RNAi as a therapeutic approach for diseases involving specific leukocyte populations.

## RESULTS AND DISCUSSION

**Preparation and Characterization of Targeted Lipid Nanoparticles (tLNPs).** To develop an effective siRNA delivery system for T cells, we have constructed siRNA-encapsulated LNPs using a microfluidic mixer system, the NanoAssemblr.[22] One of the challenges that has faced the robust scalable development of LNPs as a siRNA delivery strategy has been the production of uniform-sized particles. This usually involves time-consuming protocols including the extrusion of lipid particles through appropriately sized filters. In addition, the encapsulation of the siRNAs required the lyophilization of the lipid complexes that were than reconstituted with siRNA-containing solutions. This led to inefficient encapsulation of the siRNAs, with much of the siRNAs failing to be incorporated. The mixing of acidified siRNAs (pH 4) with a mixture of lipids (cholesterol, DSPC, PEG-DMG, Dlin-MC3-DMA, and DSPE-PEG-maleimide; Figure 1A) resulted in the production of highly uniform-sized nanoparticles (NPs) that had a mean diameter of ~58 nm measured by dynamic light scattering. Since the $pK_a$ of the Dlin-MC3-DMA lipid is 6.44, it is expected to provide a minimal or neutral charge at physiological pH (7.4), and indeed, the $\zeta$-potential of the LNPs was shown to be approximately −9 mV (Table 1). The particles' hydrodynamic diameter was also confirmed using transmission electron microscopy (TEM) (Figure 1B). We have observed close to 100% encapsulation of siRNA by RiboGreen assay; similar studies have been reported previously for LNPs prepared by the NanoAssemblr.[12,15]

To construct tLNPs, dithiothreitol (DTT)-reduced mAbs against CD4 (clone YTS.177) were chemically conjugated to the maleimide functional group incorporated on the LNPs. This procedure resulted in tLNPs with a mean diameter of ~130 nm and a $\zeta$-potential of about −10 mV (Table 1). This size was also validated using TEM (Figure 1B), and the increase in size of tLNPs could be explained by the chemical conjugation of the mAb followed by concentration of the LNPs using an Amicon centrifugal filter. siRNA encapsulation efficiency was tested using a RiboGreen assay. We observed encapsulation efficiency close to 100% since no free siRNA was detected. Antibody presence on the surface of LNPs was confirmed using a dot plot assay (Supporting Information Figure S1).

**Specific Binding of tLNPs to $CD4^+$ T Cells *ex Vivo*.** The delivery of siRNAs to specific cell populations requires the use of targeting agents, such as antibodies, peptides, or ligands that recognize cell surface antigens whose expression is restricted to or enriched on a specific cell type.[23] Importantly, for the siRNA to be delivered to the cell, the targeting agent must induce internalization of the cargo. To test whether tLNPs can

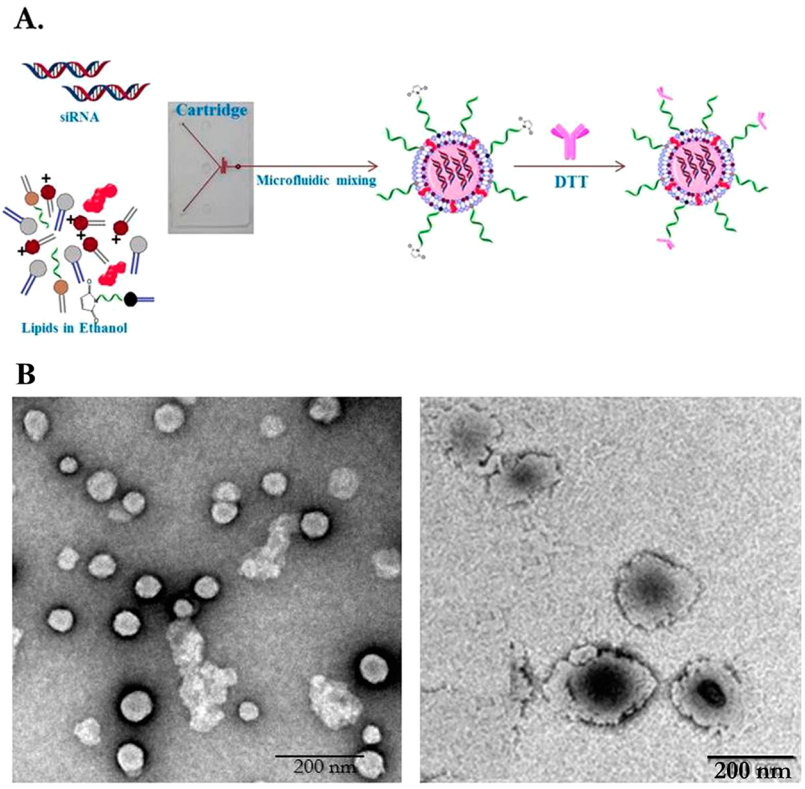


**Figure 1. Preparation and characterization of LNPs. (A) Schematic illustration of the process in which tLNPs are formed by microfluidic mixing of lipids. (B) TEM images of unconjugated LNPs (left) or tLNPs (right). Scale bar 200 nm.**

**TABLE 1. Characterization of LNPs by Dynamic Light Scattering and ζ-Potential Measurements[a]**

| | LNPs | CD4-tLNPs |
|---|---|---|
| hydrodynamic diameter (*d*, nm) | 58 ± 6 | 129 ± 5 |
| polydispersity index | 0.1 ± 0.05 | 0.12 ± 0.02 |
| ζ-potential (mV) | −9.3 ± 0.3 | −10 ± 0.5 |
| siRNA encapsulation (%) | 95 ± 2 | 95 ± 9 |

[a] Data are presented as mean ± SD of six independent preparations.

mediate specific targeting of siRNA to $CD4^+$ cells and induce internalization, tLNPs or LNPs coated with an isotype control mAb (isoLNPs) encapsulating Cy5-labeled siRNA (siCy5) were used to treat a heterogeneous population of primary C57BL/6 splenocytes *ex vivo*. To measure binding to the target cells, tLNPs (siCy5) or isoLNPs (siCy5) were incubated with heterogeneous population of splenocytes and analyzed by flow cytometry. Significant and robust binding to $CD4^+$ cells was observed for tLNP (orange dots; upper right quadrant) treated splenocytes, while no significant binding was observed for isoLNP treated splenocytes (gray dots; upper left quadrant). On the other hand, nonspecific binding to either $CD8^+$ cells or B cells (lower left quadrant) was observed for tLNP and isoLNP treated cells (Figure 2A). Representative bar graphs are shown in Figure 2B, demonstrating that a significant amount (~100%) of $CD4^+$ cells bind tLNPs compared to isoLNPs (~1%). To test the tLNP uptake, an additional stage of incubation at 37 °C for 30 min was added following tLNP binding. By confocal microscopy, we demonstrated the uptake of tLNPs into the target cells. As shown in Figure 2C, the uptake of tLNPs exclusively into $CD4^+$ cells based on co-labeling of the siCy5-containing cells with anti-CD4 PE (for membrane), calcein, and Hoechst (for cytoplasm and nuclei staining) validates tLNP internalization. tLNP specificity was also validated by labeling a $CD8^+$ T cell subset that, unlike $CD4^+$, did not demonstrate tLNP uptake (Supporting Information Figure S2). Hence, anti-CD4 mAb-coated LNPs are suitable to deliver siRNAs into $CD4^+$ cells.

**Targeted Silencing in Blood-Circulating $CD4^+$ T Cells.** To examine the capability of tLNP delivering siRNAs to silence gene expression in $CD4^+$ T cells *in vivo*, we have devised tLNP-containing siRNAs against CD45 (tLNPs (siCD45)). CD45, a cell surface tyrosine phosphatase, was chosen since it is a pan leukocyte marker and thus can be used for testing specific silencing in different leukocyte subsets. First, we tested whether tLNPs can target circulating $CD4^+$ T cells. Mice were intravenously injected with tLNPs (siCy5) or isoLNPs (siCy5) as a control. One hour post-administration, blood was harvested, stained for markers of different leukocytes subsets, and analyzed by flow cytometry. Remarkably, all $CD4^+$ cells bound tLNPs, while none of the other leukocyte subsets examined showed Cy5 labeling compared to isoLNPs or mock treated control groups

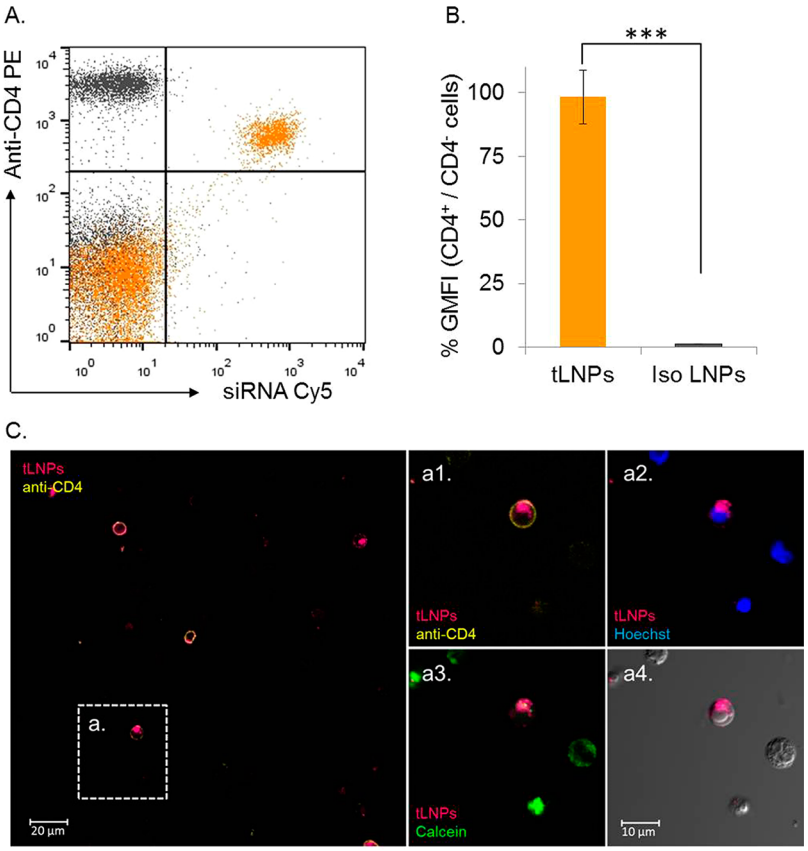


**Figure 2. tLNP binding and internalization into CD4$^+$ T cells *ex vivo*. Primary splenocytes were incubated with tLNPs (siCy5) or isoLNPs (siCy5) as a control for 30 min. CD4$^+$ cells were then labeled with anti-CD4 PE. (A) Flow cytometry dot blot analysis of gated live lymphocyte population, with orange and gray dots indicating tLNPs and isoLNPs, respectively. (B) Corresponding histograms of % GMFI (geometric mean fluorescence intensity) calculated for CD4$^+$ population over CD4$^-$ populations including CD8 and CD19 cells; data presented as mean ± SD, $n = 3$, ***$p < 0.0005$. (C) Splenocytes were incubated for another 30 min at 37 °C to allow internalization. Cells were stained with Hoechst and calcein for nuclear and cytoplasm detection followed by membrane staining with anti-CD4 AF594. Cells were analyzed by confocal microscopy for internalization (left panel); representative individual images of area (a) shown in the right panels.**

(Figure 3A). Representative bar graphs are shown in Figure 3B.

After confirming *in vivo* binding, we tested the ability of tLNPs (siCD45) to knockdown CD45 expression in C57BL/6 mice. To this end, we have used several LNPs as controls, including tLNPs that were constructed using siRNA against luciferase (tLNPs (siluc)) and isoLNPs (siCD45) or LNPs (siCD45) (unmodified LNPs). Five days post-administration, blood was harvested and cells were stained for CD45. As shown in Figure 3C, only mice treated with tLNPs (siCD45) resulted in CD45 silencing in leukocytes over the control groups. Representative histograms showing a significant reduction of CD45 levels in mice treated with tLNPs compared to isoLNPs and other control groups are presented in Figure 3D. The data presented in these experiments were performed in triplicate and reproduced with two independent experiments and with two different productions of LNPs. To test the specificity of silencing, the cells harvested from the treated animals were stained with anti-CD3 PerCP and anti-CD4 PE antibodies (Figure 3E). Remarkably, almost 100% of the silenced cells were CD4$^+$ T cells. Therefore, we achieved a very high specificity using the tLNPs in circulating CD4$^+$ T cells.

Next, we tested these tLNPs for immune toxicity. We have assayed a panel of cytokines, TNF-α, IL-17, and IL-10, in mice treated with either the tLNPs (siCD45) or LPS, a potent TLR activator, as a positive control. Only a mild elevation of cytokines was observed in tLNP (siCD45) treated mice over untreated mice (see Supporting Information Figure S3).

**tLNPs Induce Gene Silencing CD4$^+$ T Cells in Different Hematopoietic organs.** One of the challenges associated with leukocyte-targeted therapies is that in order to manipulate all leukocytes of a specific subset, such as CD4$^+$ T cells, the delivery agent needs to reach diverse organs within the body because leukocytes are distributed across multiple tissues, including spleen, lymph nodes, and bone marrow.

To determine the breadth of siRNA delivery across lymphoid tissues, we systemically examined the binding of tLNPs to CD4$^+$ T cells in different hematopoietic organs. Mice were injected intravenously with tLNPs (siCy5) or isoLNPs (siCy5). One hour post-injection, cells from the spleen, inguinal lymph nodes, and bone

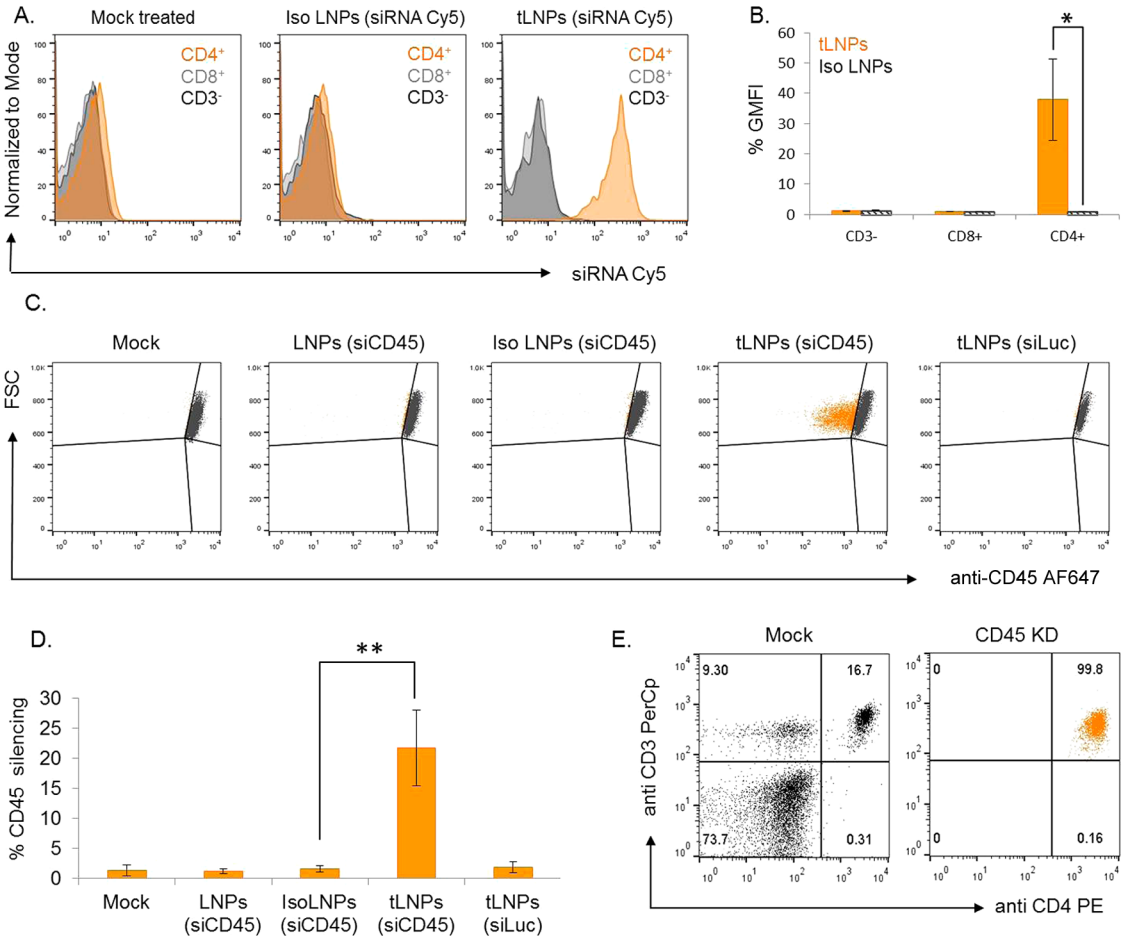


**Figure 3. tLNPs target blood-circulating CD4$^+$ T cells *in vivo* and induce gene silencing. (A) Targeting blood CD4$^+$ T cells *in vivo*. One hour post i.v. administration of tLNPs (siCy5) or isoLNPs (siCy5), circulating lymphocytes were isolated and stained with a set of antibodies (anti-CD4 PE, anti-CD3 PerCp, and anti-CD8 FITC). Representative histograms of flow cytometry analysis for LNP-binding profile in blood lymphocytes from two independent experiments are shown. (B) Corresponding bar graphs are presented as percent GMFI values over mock samples; data represent mean ± SD, $n = 3$, $*p < 0.05$. (C) tLNPs silence CD45 in blood T lymphocytes. Mice were injected with tLNPs (siCD45), saline (mock), tLNPs (siLuc), isoLNPs (siCD45), or LNPs (siCD45) as controls. Five days post i.v. administration, circulating lymphocytes were isolated and stained for CD45 expression. Flow cytometry analysis of dot blots gated for live lymphocytes; results were mean of two independent experiments, $n = 5$. (D) Corresponding histograms of percent CD45 silencing calculated from CD4 gated populations; data represent mean ± SD, $n = 5$, $**p < 0.005$. (E) CD45 is silenced specifically in CD4$^+$-circulating T cells. After 5 days administration of saline or tLNP (siCD45) circulation, lymphocytes were isolated and stained with a set of antibodies. Flow cytometry dot blot profile of CD45 silenced cell population gated for CD4$^+$/CD3$^+$ cells, $n = 5$; KD, knockdown.**

marrow were isolated and stained with a set of antibodies to detect different leukocyte subsets (anti-CD3, anti-CD4, and anti-CD8). Remarkably, all CD4$^+$ T cells from each of the tissues tested showed specific binding of the tLNPs, while no binding to any of the organs was observed in mice treated with isoLNPs (Supporting Information Figure S4). Although all of the tissues showed binding to the CD4$^+$ T cells, the binding level in different organs was heterogeneous (Supporting Information Figure S4). As shown in Figure 4A, the highest binding was observed in blood-circulating CD4$^+$ T cells, while the lowest binding was observed in lymph nodes. This heterogeneity could result from different tLNP kinetics across different tissues.

After demonstrating the selective binding of the tLNPs to CD4$^+$ T cells in all the tested organs, we sought to examine its ability to induce potent gene silencing. Five days post i.v. administration of tLNPs (siCD45), cells from blood, spleen, lymph nodes, and bone marrow were isolated and co-stained for CD45, CD3, CD8, and CD4 expression. Flow cytometry analysis of the CD3$^+$ and CD4$^+$ cell populations clearly shows specific CD45 knockdown from each of these analyzed tissues (Figure 4B). As shown in Figure 4C, the most effective silencing was observed in CD4$^+$ T cells of lymph nodes, with 36% of the cells staining negative for CD45 compared to the mock treated cells, followed by the peripheral blood (35%), spleen (31%), and bone marrow (24%). Notably, the other cell types showed no decrease in their CD45 expression levels (Supporting Information Figure S5).

To examine whether the amount of tLNP is a limiting factor, we tested the binding and silencing efficacy of tLNPs at higher tLNP doses (2 mg/kg siRNA).

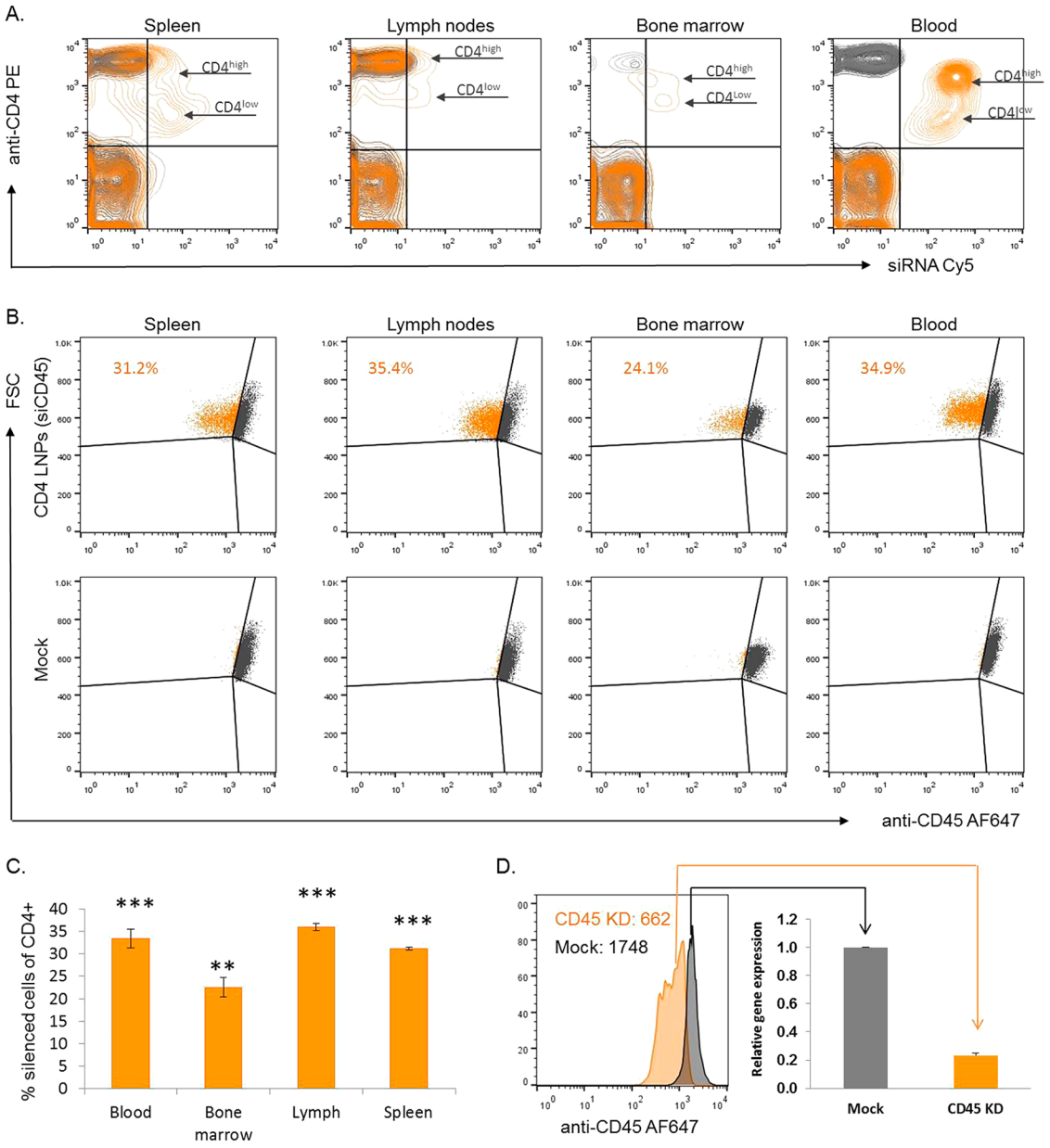


**Figure 4. tLNPs target and silence CD4$^+$ T cells in hematopoietic organs. (A) tLNP binds CD4$^+$ cells in diverse hematopoietic organs *in vivo*. One-hour post-administration of siCy5-containing tLNPs (orange) or saline (gray), spleen, lymph nodes, bone marrow, and blood lymphocytes were isolated and stained with a set of antibodies (anti-CD4 PE, anti-CD3 PerCp, and anti-CD8 FITC). Representative dot blot analysis for gated live lymphocytes is presented; data were obtained from two independent experiments, $n$ = 5 mice/group. (B) CD4 specific silencing in hematopoietic organs. Five days after administration of tLNP (siCD45) (orange) or saline (gray) administration, spleen, lymph nodes, bone marrow, and blood lymphocytes were isolated and incubated with a set of antibodies (anti-CD45 AF647, anti-CD4 PE, anti-CD3 PerCp, and anti-CD8 FITC). Representative dot blot analysis for gated live CD4$^+$ lymphocytes. (C) Corresponding bar graphs; error bars represent mean ± SD, $n$ = 5 mice/group, ***$p$ < 0.0005, **$p$ < 0.005 are compared to mock treated sample. (D) Silencing of CD45 in CD4$^+$ T cells at the mRNA level. Gated CD45$^{KD}$ and mock CD4$^+$ T cells were collected by BD FACSARIAIII cell sorter; mRNA was isolated, and CD45 mRNA levels were tested by quantitative polymerase chain reaction. All values are normalized to murine PPIB gene expression (endogenous control).**

We observed a significantly higher specific binding in blood and bone marrow (Supporting Information Figure S6A) of the mice treated with 2 mg/kg siRNA compared with the dose we frequently use (1 mg/kg). Interestingly, a functional experiment using a higher dose of tLNPs (siCD45) did not result in higher silencing. A dose response experiment using 0.5, 1, and 2 mg/kg siRNA showed a significant advantage for 1 mg/kg compared with 0.5 mg/kg in the lymph nodes, without any significant change in silencing with the 2 mg/kg dose (Supporting Information Figure S6B). To further validate siRNA silencing, CD4$^+$ T cells, CD45$^{KD}$ (KD, knockdown) cells from the spleen of the tLNP treated animals, and CD4$^+$ cells from mock treated animals were isolated by using Cell Sorter (BD FACSAriaIII). CD45 mRNA

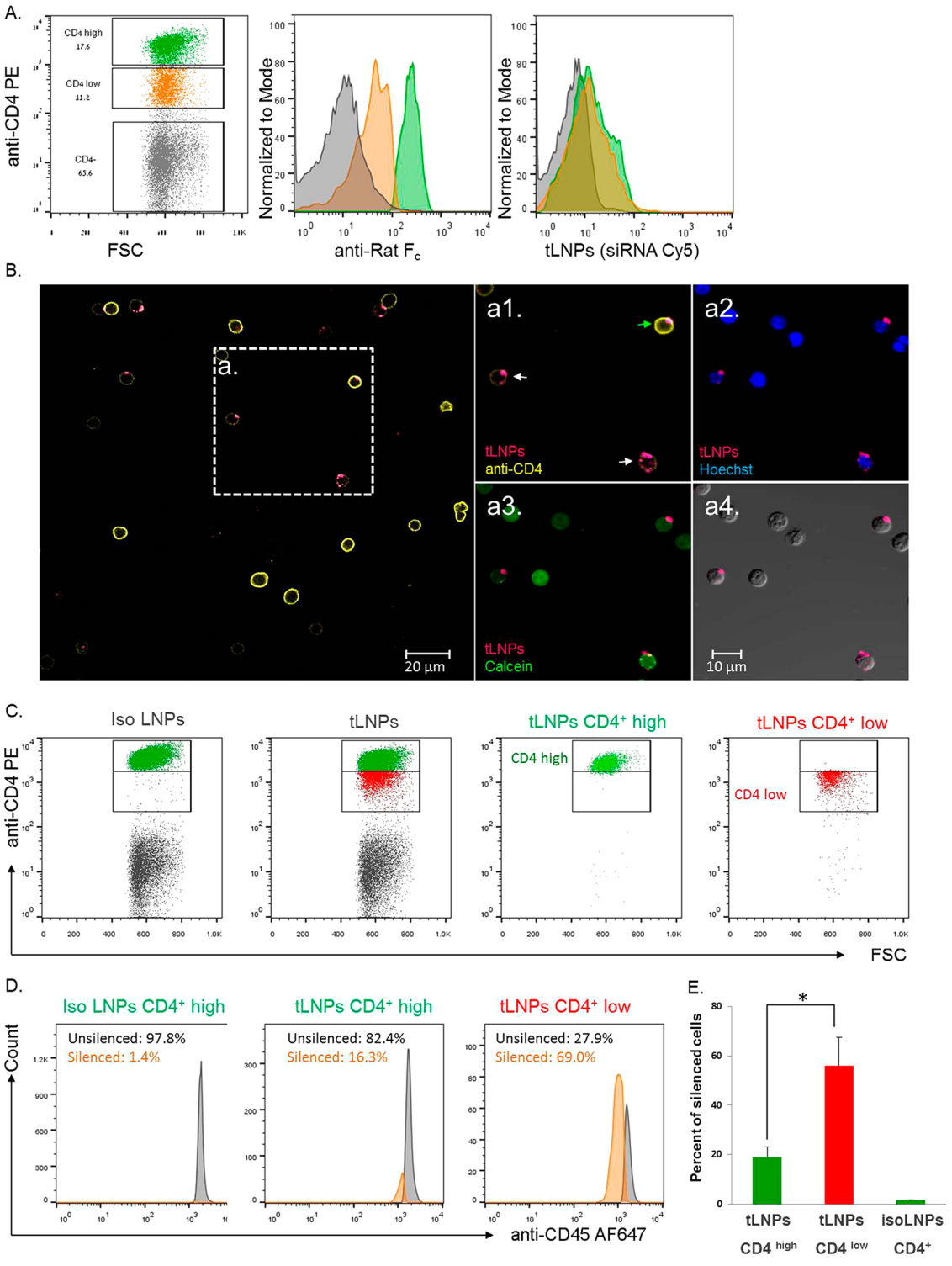


**Figure 5. LNP internalization by a CD4 subset followed by functional silencing. (A) One hour post-tLNP (siCy5) administration, splenocytes were isolated, stained with anti-rat Fc, followed by anti-CD4 PE, and analyzed by flow cytometry; analysis is presented on gated populations. (B) Splenocytes collected from tLNP (siCy5) treated mice were stained with Hoechst, calcein, and anti-CD4 PE. Cells were analyzed by confocal microscopy. $CD4^{high}$ and $CD4^{low}$ cells are marked with green and white arrows, respectively. (C). One hour post-administration of tLNPs or isoLNPs (siCD45), splenocytes were collected and labeled with anti-CD4 PE. $CD4^{+}$ T cells of isoLNPs, $CD4^{high}$ (green), and $CD4^{low}$ (red) cells of tLNPs were separated using BD FACSAriaIII cell sorter. (D) Sorted cells were cultured *in vitro* for 3 days, then stained with anti-CD45 AF647 and analyzed by flow cytometry. (E) Corresponding bar graphs; error bars represent mean ± SD, $n = 3$ mice/group, $*p = 0.006$.**

expression levels were analyzed by quantitative real-time polymerase chain reaction (qRT-PCR). As shown in Figure 4D, a significant (~80%) decrease in CD45 mRNA levels was observed in $CD4^{+}$ T cells collected

from tLNP treated mice compared with mock treated $CD4^+$ T cells.

**tLNPs Are Internalized by a Distinct CD4 Subset Followed by Functional Silencing.** After establishing tLNPs as a platform strategy to specifically silence genes of interest using siRNAs in circulating and resting $CD4^+$ T lymphocytes (using the pan leukocyte surface marker CD45 as a gene model), we tried to decipher the mechanism that underlies the differences between the two $CD4^+$ T cell populations that differ in their response to the tLNPs. One demonstrates CD45 silencing, and the other does not alter its CD45 expression levels. Intriguingly, two distinct $CD4^+$ T cell populations were noticed in all tissues tested in binding experiments after 1 h (Figure 4A) or 4 h (Supporting Information Figure S5B) after tLNP administration. One shows high CD4 PE staining, as in mock cells ($CD4^{high}$), and the other presents low CD4 PE staining ($CD4^{low}$). $CD4^{low}$ population represents $CD4^+$ T cells and not a different population of cells since this population of cells stained positively for the T cell co-receptor CD3 encompassing both the $CD4^{high}$ and $CD4^{low}$ cell populations (Supporting Information Figure S7). This $CD4^{low}$ population of cells was not found in the untreated mice. Since the percent of the $CD4^{low}$ population resembled the silencing percent that we obtained in the silencing assays, we wanted to test whether the reduction in anti-CD4 PE can be a result of CD4 receptor sequestering from the membrane due to tLNP internalization, followed by silencing. To determine if there was a correlation between low CD4 surface expression and tLNP internalization, the level of internalized tLNPs (siCy5) was tested by both flow cytometry and confocal microscopy analysis. For flow cytometer assay, we have used a secondary antibody (anti-rat Fc) directed against the fragment crystallizable (Fc) region of the CD4 mAb of tLNPs. This experimental method is not designed to detect internalizing particles but rather cell-surface-bound particles. Flow cytometry analysis clearly demonstrates that, although the amount of siCy5 is similar between $CD4^{low}$ and $CD4^{high}$ cells, $CD4^{low}$ population has less tLNPs on the surface because $CD4^{low}$ has reduced staining of anti-rat Fc compared to that of the $CD4^{high}$ population (Figure 5A). These results were validated by confocal microscopy, in which cytoplasm, nuclei, and CD4 membrane were stained with calcein, Hoechst, and anti-CD4, respectively, to ensure tLNP cytoplasmic localization. As shown in Figure 5B, $CD4^{low}$ cells have effectively internalized the tLNPs (siCy5); on the other hand, $CD4^{high}$ cells had lower levels of internalized tLNPs (siCy5) with the majority of tLNPs located on the surface (Figure 5B). Therefore, these results demonstrate that two populations of $CD4^+$ cells ($CD4^{low}$ and $CD4^{high}$ cells) in the tLNP treated samples may reflect the degree of internalization and sequestration of the CD4 molecules. This could suggest that there may be differences between $CD4^+$ cell populations in their ability to endocytose the tLNPs and may explain the CD45 knockdown efficiency as seen in Figure 4B.

Next, we wanted to confirm that $CD4^{low}$ cells internalize the tLNPs and that this internalization leads to silencing. This will determine that the bottleneck for gene silencing in CD4 cells using tLNPs system is the internalization step. For this purpose, we have designed an experiment in which $CD4^{low}$ and $CD4^{high}$ populations are separated by FACS Sorter (Figure 5C), 1 h after administration of tLNPs (siCD45) *in vivo*, and CD45 expression levels are tested after 3 days in culture. As a control, we sorted $CD4^+$ cells from mice treated with isoLNPs (siCD45), in which no $CD4^{low}$ population was observed. Remarkably, up to 70% silencing was observed in $CD4^{low}$ populations compared with 16% in $CD4^{high}$ population. Neglected 2% silencing was observed in the $CD4^{high}$ population of the isoLNP treated group (Figure 5E).

Revealing that $CD4^{low}$ is the silenced population also contributes to deciphering how lymph node $CD4^+$ T cells exhibit high knockdown efficacy while showing the lowest tLNP uptake. Following uptake of the particles at the single-cell level is limited when using siCy5 due to degradation of the florescence dye along with florescence decay due to low endosomal pH. Indeed, Cy5 labeling is dramatically decreased among all tissues 4 h post-administration (Supporting Information Figure S8A); however, since $CD4^{low}$ represents the silenced cells that internalize the tLNPs, we can follow their fate. Interestingly, after 4 h, we can detect a significant increase of ~5.5% in $CD4^{low}$ in lymph nodes accompanied by a trend of a $CD4^{low}$ decrease in other tissues (Supporting Information Figure S8B). This might imply that more tLNPs accumulate in the lymph after 4 h or that CD4 cells have migrated to the lymph.

It is well-accepted that the main obstacle for effective gene silencing by siRNA delivery systems resides in siRNA endosome escape. However, our findings shed new light on internalization as the bottleneck of T-cell-targeted siRNA delivery. Further understating the mechanisms that enable tLNP internalization in $CD4^{low}$ population may improve efficacy and gene silencing by siRNA delivery platforms.

## CONCLUSIONS

We have devised a strategy to specifically target and silence gene expression in $CD4^+$ T cells. We have shown here that our system can effectively silence CD45 in $CD4^+$ T cells at much lower doses (1 mg/kg body) than any published nontargeted system to leukocytes, and that this silencing was detected in all the major tissues that harbor T cells (blood, spleen, bone marrow, and inguinal lymph nodes). Moreover, CD45 silencing was restricted to the $CD4^+$ T cells and was not observed in other lymphocyte subsets. This decrease in CD45 expression was shown at both the

protein and mRNA levels. Interestingly, we noticed that all $CD4^+$ cells were targeted by the tLNPS (siCD45); there was a $CD4^+$ T cell subset in which uptake of the tLNPs was less efficient. To further elucidate this phenomenon, we conducted a series of experiments focusing on the cellular penetration of the tLNPs to $CD4^+$ cells. Our results demonstrate that there were two distinct $CD4^+$ T cell populations that differ in their tLNP uptake ability. Distinct population of $CD4^+$ T cells ($CD4^{low}$) was permissive for tLNP internalization followed by siRNA cytoplasmic diffusion, while the remaining $CD4^+$ T cells harbor tLNPs ($CD4^{high}$) on their surface without proceeding to internalization. Interestingly, we have shown that tLNP internalization and not endosome escape is a central event that defines tLNP efficacy and that this tLNP internalization takes place only 1 h post-systemic tLNP administration. Further research focusing on deciphering the limitation of $CD4^{high}$ population to internalize tLNPs will enable one to maximize gene silencing in T lymphocytes.

## MATERIALS AND METHODS

**Materials.** *Monoclonal Antibodies.* FITC anti-mouse CD8 (clone 5H10-1), PerCP anti-mouse CD3 (clone 145-2C11), PE anti-mouse CD19 (clone 6D5), and PE anti-mouse CD4 (clone GK1.5) were purchased from BioLegend. Anti-mouse CD4 (clone YTS.177) and rat IgG2a isotype (clone 2A3) were purchased from bioxcell.

Secondary antibody Alexa Fluor 647 AffinityPure F(ab′)2 fragment donkey anti-rat IgG (H+L) (minimal cross-reaction to mouse) was purchased from Jackson ImmunoResearch Laboratories.

*Lipids.* Cholesterol, DSPC, and DSPE PEG-Mal were obtained from Avanti Polar Lipids, USA. The ionizable lipid Dlin-MC3-DMA was synthesized according to previously described method.[15]

Chemically modified siRNAs against CD45 were synthesized at Alnylam Pharmaceuticals (Cambridge, MA) using standard phosphoramidite chemistry.

CD45 siRNA:
sense strand: cuGGcuGAAuuucAGAGcAdTsdT
anti-sense strand: UGCUCUGAAAUUcAGCcAGdTsdT
Luc siRNA:
sense strand: cuuAcGcuGAGuAcuucGAdTsdT
anti-sense strand: UCGAAGuACUcAGCGuAAGdTsdT

2′-OMe-modified nucleotides are in lower case, and phosphorothioate linkages are represented by "s".

**Preparation of Lipid-Based Nanoparticles Entrapping siRNAs.** LNPs were prepared by using microfluidic micro mixture (Precision NanoSystems, Vancouver, BC) as previously described.[15] Briefly, one volume of lipid mixtures (MC3, DSPC, Chol, DMG-PEG, and DSPE-PEG Mal at 50:10:38:1.5:0.5 mol ratio) in ethanol and three volumes of siRNA (1:16 w/w siRNA to lipid) containing acetate buffer solutions were mixed by using dual syringe pump (model S200, kD Scientific, Holliston, MA) to drive the solutions through the micro mixer at a combined flow rate of 2 mL/min (0.5 mL/min for ethanol and 1.5 mL/min for aqueous buffer). The resultant mixture was dialyzed against phosphate buffered saline (PBS) (pH 7.4) for 16 h to remove ethanol. For Cy5-labeled particles, 10% Cy5-labeled nontargeted siRNA was used.

**siRNA Entrapment Efficiency.** siRNA encapsulation efficiency was determined by the Quant-iT RiboGreen RNA assay (Life Technology) as previously described by us and others.[12] Briefly, the encapsulation efficiency was determined using RNA binding dye RiboGreen by comparing fluorescence between LNPs and tLNPs in the presence and absence of Triton X-100. In the absence of detergent, fluorescence can be measured from accessible (free or surface-bound) siRNA only, whereas in the presence of detergent, fluorescence is measured from total siRNA; thus, the % encapsulation is described by the following equation:

$$\%\text{siRNA encapsulation} = [1 - (\text{free siRNA concn}/\text{total siRNA concn})] \times 100$$

**Conjugation of Anti-CD4 Antibodies with LNPs (tLNPS).** CD4 IgG (clone YTS 177) or Isotype mAbs (clone X63) were reduced with 1 mM DTT for 30 min at room temperature. DTT was removed by using 7K cutoff Zeba spin desalting columns (Thermo, USA) according to the manufacturer's protocol. Maleimide-functionalized LNPs were added and incubated for 1 h at room temperature and overnight at 4 °C. To remove unconjugated antibody, LNPs were loaded on sepharose CL4b beads and purified by gel filtration chromatography using PBS as the mobile phase. LNP fractions were collected and concentrated by 10K Amicon tubes (Millipore).

**Size Distribution and ζ-Potential Measurements.** The size and ζ-potential of LNPs were measured by dynamic light scattering using Malvern nano-ZS Zetasizer (Malvern Instruments Ltd., Worcestershire, UK). Size and ζ-potential measurements were performed in water.

**Transmission Electron Microscopy Analysis.** A drop of aqueous solution containing LNPs (with or without mAbs) was placed on the carbon-coated copper grid and dried. The morphology of LNPs was analyzed by a JEOL 1200 EX (Japan) transmission electron microscope.

**Dot Blot Analysis.** Several concentrations of rat anti-CD4 (clone YTS.177) along with LNPs, tLNPs, and isoLNPs were blotted on a nitrocellulose membrane. After blocking in 5% low-fat milk, the membrane was incubated with AffiniPure $F(ab')_2$ fragment anti-rat conjugated to horseradish peroxidase (Jackson ImmunoResearch) for 30 min at room temperature. ECL (Thermo Scientific Pierce) was used as a substrate solution.

***In Vitro* Cellular Uptake.** Freshly isolated splenocytes were incubated for 30 min at 4 °C with tLNPs (siCy5) followed by washing with PBS and incubation for 30 min at 37 °C to allow internalization. Afterward, cells were stained with anti-CD4 PE and anti-CD8 FITC. Cells were then analyzed by a Nikon confocal microscope.

***In Vivo* tLNP Biodistribution.** Mice were intravenously injected with tLNPs (siCy5) at 1 mg/kg siRNA per body weight of mouse. After 1 h, mice were sacrificed to collect blood, spleen, lymph nodes, and bone marrow cells.

*Isolation of Lymphocytes.* Blood was collected in heparin-coated collection tubes, and the leukocytes were isolated by density centrifugation using ficoll paque plus (GE Healthcare). Single-cell suspensions of splenocytes were prepared by mincing of spleens and passing through a 70 μm cell strainer (BD Bioscience). Red blood cells were lysed using ACK lysis buffer, and the resulting cells were resuspended in PBS. Inguinal lymph nodes were isolated and minced to make a single-cell suspension. Cells were washed twice with PBS followed by passing through a 70 μm cell strainer. Cells were stained with a secondary Alexa Fluor 647 conjugated anti-rat Fc antibody at 4 °C for 30 min; tLNPs were detected on the surface of the cells by Alexa Fluor 647 anti-rat Fc and/or by Cy5. Cells were then washed with PBS containing 1% fetal bovine serum and incubated with labeled anti-CD4, CD8, and CD3 antibodies for 30 min at 4 °C. Cells were washed and analyzed on a Becton Dickinson FACScalibur flow cytometer with CellQuest software (Becton Dickinson, Franklin Lakes, NJ). Data analysis was performed using FlowJo software (Tree Star, Inc., OR, USA). In addition, cells were imaged on a Nikon confocal microscope.

**Confocal Microscopy Analysis.** One hour post-administration of tLNPs, splenocytes were collected as mentioned above and stained with Hoechst (nucleus) and calcein (cytoplasm) labeling followed by anti-CD4 PE for membrane staining. Cells were

washed, and images were taken with a Nikon C2 (Nikon Instruments Inc., USA) confocal microscope.

***In Vivo* Silencing.** Six to 8 week old C57BL6/J mice were obtained from the Animal Breeding Center, Tel Aviv University (Tel Aviv, Israel). All animal protocols were approved by the Tel Aviv Institutional Animal Care and Use Committee. Mice were maintained and treated according National Institutes of Health guidelines. tLNPs or isotype LNPs containing siRNA against CD45 or luciferase were injected intravenously (1 mg/kg siRNA). Mice were euthanized after 5 days, and organs were collected for further analysis.

**Cell Sorting and qPCR.** Five days later, tLNPs (siCD45) were injected and splenocytes were isolated and stained with anti-CD4 PE and anti-CD45 AF647. As a control, mock treated splenocytes were stained with anti-CD4 PE. $CD4^+$ and $CD45^{low}$ populations from tLNP treated mice were collected, and $CD4^+$ cells were collected from mock sample mice as a control with FACSARIA (BD). mRNA was isolated using EZ-RNA (Biological Industries, Israel), and cDNA was prepared using a cDNA synthesis kit (Quanta Biosciences) mouse PPIB was used as the endogenous control. Primer sequences: mPPIB FW: 5′ CCA TCG TGT CAT CAA GGA CTT C 3′; mPPIB Rev: 5′ GAT GCT CTT TCC TCC TGT GCC 3′; mCD45 FW: 5′ TCT TAC ACC ATC CAC TCT GGG C 3′; mCD45 Rev: 5′ GCT TCG TTG TGG TAG CTA TGG TT 3′.

***In Vivo* Immune Activation.** LNPs were injected intravenously into C57BL mice. Lipopolysaccharide (LPS, Sigma) at a concentration of 1 mg/mL (100 $\mu$L) was used as a positive control. Blood was collected 2 h after injection. Serum was separated and stored at −80 °C prior to cytokine analysis. Serum samples were analyzed for cytokine levels according to the manufacturer's protocol using the Milliplex MAP kit (Millipore). The quantification was done based on standard curves for each cytokine.

**Statistical Analysis.** All data were expressed mean ± SD. Statistical analysis was performed using two-sided student's *t* test. Differences between or among groups are labeled as n.s. for not significant, * for $p < 0.05$, ** for $p < 0.005$, and *** for $p < 0.0005$.

*Conflict of Interest:* The authors declare the following competing financial interest(s): D.P. has financial interest in Quiet Therapeutics. A.G.S. is an employee of Alnylam Pharmaceuticals. The rest of the authors declare no competing financial interest.

*Supporting Information Available:* Dot blot analysis, *in vivo* immune activation, *in vivo* biodistribution study of LNPs, dose-dependent biodistribution, and silencing of tLNPs. The Supporting Information is available free of charge on the ACS Publications website at DOI: 10.1021/acsnano.5b02796.

*Acknowledgment.* S.R. thanks Tel Aviv University Center for Nanoscience and Nanotechnology for an excellence postdoctoral fellowship. Daniel Rosenblum and Sefora Conti are acknowledged for their help in confocal images and dot blot analysis. Fabio Arrojo is acknowledged for help with the abstract graphic. This work was supported in part by grants from the NIH (1R33AI088601), the Israeli Centre of Research Excellence (I-CORE), Gene Regulation in Complex Human Disease, Center No 41/11; FTA: Nanomedicine for Personalized Theranostics, The Leona M. and Harry B. Helmsley Nanotechnology Research Fund; ERC consolidator grant (LeukoTheranostics) to D.P.

## REFERENCES AND NOTES

1. Peer, D. A Daunting Task: Manipulating Leukocyte Function with RNAi. *Immunol. Rev.* **2013**, *253*, 185–197.
2. Gust, T. C.; Neubrandt, L.; Merz, C.; Asadullah, K.; Zugel, U.; von Bonin, A. RNA Interference-Mediated Gene Silencing in Murine T Cells: *In Vitro* and *In Vivo* Validation of Proinflammatory Target Genes. *Cell Commun. Signaling* **2008**, *6*, 3.
3. Freeley, M.; Long, A. Advances in siRNA Delivery to T-Cells: Potential Clinical Applications for Inflammatory Disease, Cancer and Infection. *Biochem. J.* **2013**, *455*, 133–147.
4. Goffinet, C.; Keppler, O. T. Efficient Nonviral Gene Delivery into Primary Lymphocytes from Rats and Mice. *FASEB J.* **2006**, *20*, 500–502.
5. Peer, D. Induction of Therapeutic Gene Silencing in Leukocyte-Implicated Diseases by Targeted and Stabilized Nanoparticles: A Mini-Review. *J. Controlled Release* **2010**, *148*, 63–68.
6. Perise-Barrios, A. J.; Jimenez, J. L.; Dominguez-Soto, A.; de la Mata, F. J.; Corbi, A. L.; Gomez, R.; Munoz-Fernandez, M. A. Carbosilane Dendrimers as Gene Delivery Agents for the Treatment of HIV Infection. *J. Controlled Release* **2014**, *184*, 51–57.
7. Tezgel, A. O.; Gonzalez-Perez, G.; Telfer, J. C.; Osborne, B. A.; Minter, L. M.; Tew, G. N. Novel Protein Transduction Domain Mimics as Nonviral Delivery Vectors for siRNA Targeting NOTCH1 in Primary Human T Cells. *Mol. Ther.* **2013**, *21*, 201–209.
8. Lee, J.; Yun, K. S.; Choi, C. S.; Shin, S. H.; Ban, H. S.; Rhim, T.; Lee, S. K.; Lee, K. Y. T Cell-Specific siRNA Delivery Using Antibody-Conjugated Chitosan Nanoparticles. *Bioconjugate Chem.* **2012**, *23*, 1174–1180.
9. Zhou, J.; Neff, C. P.; Swiderski, P.; Li, H.; Smith, D. D.; Aboellail, T.; Remling-Mulder, L.; Akkina, R.; Rossi, J. J. Functional *In Vivo* Delivery of Multiplexed Anti-HIV-1 siRNAs via a Chemically Synthesized Aptamer with a Sticky Bridge. *Mol. Ther.* **2013**, *21*, 192–200.
10. Neff, C. P.; Zhou, J.; Remling, L.; Kuruvilla, J.; Zhang, J.; Li, H.; Smith, D. D.; Swiderski, P.; Rossi, J. J.; Akkina, R. An Aptamer-siRNA Chimera Suppresses HIV-1 Viral Loads and Protects from Helper CD4(+) T Cell Decline in Humanized Mice. *Sci. Transl. Med.* **2011**, *3*, 66ra6.
11. Kim, S. S.; Peer, D.; Kumar, P.; Subramanya, S.; Wu, H.; Asthana, D.; Habiro, K.; Yang, Y. G.; Manjunath, N.; Shimaoka, M.; Shankar, P. RNAi-Mediated CCR5 Silencing by LFA-1-Targeted Nanoparticles Prevents HIV Infection in BLT Mice. *Mol. Ther.* **2010**, *18*, 370–376.
12. Peer, D.; Park, E. J.; Morishita, Y.; Carman, C. V.; Shimaoka, M. Systemic Leukocyte-Directed siRNA Delivery Revealing Cyclin D1 as an Anti-inflammatory Target. *Science* **2008**, *319*, 627–630.
13. Peer, D.; Zhu, P.; Carman, C. V.; Lieberman, J.; Shimaoka, M. Selective Gene Silencing in Activated Leukocytes by Targeting siRNAs to the Integrin Lymphocyte Function-Associated Antigen-1. *Proc. Natl. Acad. Sci. U.S.A.* **2007**, *104*, 4095–4100.
14. Gilleron, J.; Querbes, W.; Zeigerer, A.; Borodovsky, A.; Marsico, G.; Schubert, U.; Manygoats, K.; Seifert, S.; Andree, C.; Stoter, M.; et al. Image-Based Analysis of Lipid Nanoparticle-Mediated siRNA Delivery, Intracellular Trafficking and Endosomal Escape. *Nat. Biotechnol.* **2013**, *31*, 638–646.
15. Cohen, Z. R.; Ramishetti, S.; Peshes-Yaloz, N.; Goldsmith, M.; Wohl, A.; Zibly, Z.; Peer, D. Localized RNAi Therapeutics of Chemoresistant Grade IV Glioma Using Hyaluronan-Grafted Lipid-Based Nanoparticles. *ACS Nano* **2015**, *9*, 1581–1591.
16. Tam, Y. Y.; Chen, S.; Cullis, P. R. Advances in Lipid Nanoparticles for siRNA Delivery. *Pharmaceutics* **2013**, *5*, 498–507.
17. Chen, S.; Tam, Y. Y.; Lin, P. J.; Leung, A. K.; Tam, Y. K.; Cullis, P. R. Development of Lipid Nanoparticle Formulations of siRNA for Hepatocyte Gene Silencing Following Subcutaneous Administration. *J. Controlled Release* **2014**, *196*, 106–112.
18. Song, E.; Lee, S. K.; Wang, J.; Ince, N.; Ouyang, N.; Min, J.; Chen, J.; Shankar, P.; Lieberman, J. RNA Interference Targeting Fas Protects Mice from Fulminant Hepatitis. *Nat. Med.* **2003**, *9*, 347–351.
19. Novobrantseva, T. I.; Borodovsky, A.; Wong, J.; Klebanov, B.; Zafari, M.; Yucius, K.; Querbes, W.; Ge, P.; Ruda, V. M.; Milstein, S.; et al. Systemic RNAi-Mediated Gene Silencing in Nonhuman Primate and Rodent Myeloid Cells. *Mol. Ther. Nucleic Acids* **2012**, *1*, e4.
20. He, W.; Bennett, M. J.; Luistro, L.; Carvajal, D.; Nevins, T.; Smith, M.; Tyagi, G.; Cai, J.; Wei, X.; Lin, T. A.; et al. Discovery of siRNA Lipid Nanoparticles To Transfect Suspension Leukemia Cells and Provide *In Vivo* Delivery Capability. *Mol. Ther.* **2014**, *22*, 359–370.

21. Jayaraman, M.; Ansell, S. M.; Mui, B. L.; Tam, Y. K.; Chen, J.; Du, X.; Butler, D.; Eltepu, L.; Matsuda, S.; Narayanannair, J. K.; et al. Maximizing the Potency of siRNA Lipid Nanoparticles for Hepatic Gene Silencing *in Vivo*. *Angew. Chem., Int. Ed.* **2012**, *51*, 8529–8533.
22. Belliveau, N. M.; Huft, J.; Lin, P. J.; Chen, S.; Leung, A. K.; Leaver, T. J.; Wild, A. W.; Lee, J. B.; Taylor, R. J.; Tam, Y. K.; et al. Microfluidic Synthesis of Highly Potent Limit-Size Lipid Nanoparticles for *In Vivo* Delivery of siRNA. *Mol. Ther. Nucleic Acids* **2012**, *1*, e37.
23. Peer, D.; Karp, J. M.; Hong, S.; Farokhzad, O. C.; Margalit, R.; Langer, R. Nanocarriers as an Emerging Platform for Cancer Therapy. *Nat. Nanotechnol.* **2007**, *2*, 751–760.